Title

Multi-kinase compensation rescues EGFR knockout in a cell line model of head and neck squamous cell carcinoma.

Authors

Ludwig, Megan

Michmerhuizen, Nicole

Wang, Jiayu

et al.

Publication Date

2023-12-01

DOI

10.1016/j.archoralbio.2023.105822

Peer reviewed

HHS Public Access

Author manuscript

Arch Oral Biol. Author manuscript; available in PMC 2024 June 27.

Published in final edited form as:

Arch Oral Biol. 2023 December ; 156: 105822. doi:10.1016/j.archoralbio.2023.105822.

Multi-kinase compensation rescues EGFR knockout in a cell line model of Head and Neck Squamous Cell Carcinoma

Megan L. Ludwig[*],
Department of Otolaryngology – Head and Neck Surgery, University of Michigan Medical School, Ann Arbor, Michigan 48109; Program in Cellular and Molecular Biology, University of Michigan Medical School, Ann Arbor, Michigan 48109

Nicole L. Michmerhuizen[*],
Department of Pharmacology, University of Michigan Medical School, Ann Arbor, Michigan 48109; Department of Otolaryngology – Head and Neck Surgery, University of Michigan Medical School, Ann Arbor, Michigan 48109

Jiayu Wang,
Department of Pharmacology, University of Michigan Medical School, Ann Arbor, Michigan 48109; Department of Otolaryngology – Head and Neck Surgery, University of Michigan Medical School, Ann Arbor, Michigan 48109

Andrew C. Birkeland,
Department of Otolaryngology – Head and Neck Surgery, University of Michigan Medical School, Ann Arbor, Michigan 48109

Behirda Karaj,
Department of Pharmacology, University of Michigan Medical School, Ann Arbor, Michigan 48109

Sai Nimmagadda,
Department of Otolaryngology – Head and Neck Surgery, University of Michigan Medical School, Ann Arbor, Michigan 48109

Jingyi Zhai,
Department of Biostatistics, University of Michigan School of Public Health, Ann Arbor, MI 48109

Apurva Bhangale,
Department of Otolaryngology – Head and Neck Surgery, University of Michigan Medical School, Ann Arbor, Michigan 48109

Aditi Kulkarni,
Department of Otolaryngology – Head and Neck Surgery, University of Michigan Medical School, Ann Arbor, Michigan 48109

Hui Jiang,
Rogel Cancer Center, University of Michigan Medical School, Ann Arbor, Michigan 48109; Department of Biostatistics, University of Michigan School of Public Health, Ann Arbor, MI 48109

Correspondance: J Chad Brenner Ph.D., 1150 E. Medical Center Drive, 9301B MSRB3, Ann Arbor, MI 48109-0602, Fax: 734-764-0014, chadbren@umich.edu.
[*]Authors contributed equally

Paul L. Swiecicki,
Department of Hematology Oncology, University of Michigan Medical School, Ann Arbor, Michigan 48109; Rogel Cancer Center, University of Michigan Medical School, Ann Arbor, Michigan 48109

J. Chad Brenner
Department of Pharmacology, University of Michigan Medical School, Ann Arbor, Michigan 48109; Program in Cellular and Molecular Biology, University of Michigan Medical School, Ann Arbor, Michigan 48109; Rogel Cancer Center, University of Michigan Medical School, Ann Arbor, Michigan 48109

Abstract

Background: Head and neck squamous cell carcinoma (HNSCC) is a debilitating disease with poor survival rates. While the epidermal growth factor receptor (EGFR)-targeting antibody Cetuximab is approved for treatment, responses are limited and the molecular mechanisms driving resistance remain incompletely understood.

Methods: To better understand how cells survive without EGFR activity, we developed an *EGFR* knockout derivative of the UM-SCC-92 cell line using CRISPR/Cas9 technology. We then characterized changes to the transcriptome with RNAseq and changes in response to kinase inhibitors with resazurin cell viability assays. Finally, we tested if inhibitors with activity in the EGFR knockout model also had synergistic activity in combination with EGFR inhibitors in either wild type UM-SCC-92 cells or a known Cetuximab-resistant model.

Results: Functional and molecular analysis showed that knockout cells had decreased cell proliferation, upregulation of *FGFR1* expression, and an enhanced mesenchymal phenotype. In fact, expression of common EMT genes including *VIM*, *SNAIL1*, *ZEB1* and *TWIST1* were all upregulated in the *EGFR* knockout. Surprisingly, *EGFR* knockout cells were resistant to FGFR inhibitor monotherapies, but sensitive to combinations of FGFR and either XIAP or IGF-1R inhibitors. Accordingly, both wild type UM-SCC-92 and Cetuximab-resistant UM-SCC-104 cells with were sensitive to combined inhibition of EGFR, FGFR and either XIAP or IGF-1R.

Conclusions: These data offer insights into EGFR inhibitor resistance and show that resistance to EGFR knockout likely occurs through a complex network of kinases. Future studies of cetuximab-resistant HNSCC tumors are warranted to determine if this EMT phenotype and/or multi-kinase resistance is observed in patients.

Introduction

Head and neck squamous cell carcinoma (HNSCC) is the 6th most common cancer by incidence worldwide, and affects more than 800,000 patients each year (Leemans et al., 2011). Most patients present with locally advanced disease and are cured with multimodality therapy including surgery, radiation, and cytotoxic chemotherapy. Unfortunately, many patients develop recurrent or metastatic disease, which is frequently incurable. In these cases, systemic therapy is the cornerstone of therapy and includes cytotoxic chemotherapeutics, immune checkpoint inhibitors, and EGFR directed therapy. Despite the development of immune checkpoint inhibitors, survival has improved only

marginally and remains poor with an average survival of approximately one year (Burtness, Harrington, et al., 2019). Development of novel approaches to overcome drug resistance is of crucial importance given the limited treatments and dismal outcomes.

With the elucidation of the genomic landscape of HNSCC, targeted therapy was recognized as being more complex than originally hoped given the lack of driver mutation events (Cancer Genome Atlas, 2015). EGFR has long been known to be overexpressed in the majority HNSCC and thought to be a rational candidate for targeted therapy. Cetuximab, an anti-EGFR chimeric monoclonal antibody, improved outcomes in combination with chemotherapy or as a single agent in recurrent/metastatic HNSCC (Vermorken et al., 2008; Vermorken et al., 2007), and is FDA approved for use in recurrent/metastatic HNSCC. However, anti-tumor responses were seen in the minority of patients and limited in duration. Subsequent studies of other small molecule EGFR inhibitors and monoclonal antibodies including afatinib, erlotinib, panitumumab, and zalutumumab have shown limited efficacy in patients with HNSCC (Brondum et al., 2018; Burtness, Haddad, et al., 2019; Siano et al., 2017; Siu et al., 2007). Despite these limitations, Cetuximab has been shown to alter the tumor immune microenvironment, antibody-dependent cellular cytotoxicity (ADCC) activity, and cytotoxic T-lymphocyte (CTL) infiltration into the tumor, anti-angiogenesis activity (Okuyama et al., 2023; Smith et al., 2023). Recognizing the limited activity of single agent EGFR inhibitor, attention has been turned to combinatorial approaches potentially leveraging alternative compensatory pathways mediating EGFR treatment resistance.

Indeed, several recent important studies have highlighted the role of various individual receptor tyrosine kinase and cell signaling pathways that are elevated in during HNSCC progression and have potential to drive Cetuximab resistance. For example, in the study by Raj et. al., the authors highlight the important role of the HGH/cMET axis in HNSCC (Raj et al., 2022) and its role in driving cetuximab resistance in many patients (Hartmann et al., 2016). Likewise, the recent identification of *HRAS* mutations in HNSCC identified a genetic driver of resistance that occurs in 5-8% of HNSCC patients (Wang et al., 2023). As such, while some cell signaling and genetic mechanisms are becoming established, the global mechanisms of resistance remain unclear.

With the clear molecular basis for EGFR inhibition in HNSCC and the ongoing challenges that have limited the efficacy of cetuximab and other EGFR-targeting therapies, research efforts by our group and others have sought to understand mechanisms of resistance to EGFR inhibition such that more effective dual-therapies could be developed. These studies have largely used therapeutics-based approaches to identify mechanisms of resistance and have shown that activation of the PI3K signaling pathway can bypass EGFR inhibition and that combined targeting of PI3K and EGFR is synergistic in HNSCCs (Anisuzzaman et al., 2017; D'Amato et al., 2014; Lattanzio et al., 2015; Michmerhuizen et al., 2016; Michmerhuizen et al., 2019; Rebucci et al., 2011; Silva-Oliveira et al., 2017; Young et al., 2013). Additional data has nominated compensatory FGFR, IGF-1R, and/or MET signaling as possible mechanisms of compensatory resistance to EGFR inhibition (Dieci et al., 2013; Goke et al., 2015; Guix et al., 2008; Jameson et al., 2011; Koole et al., 2016; Michmerhuizen et al., 2022; Quintanal-Villalonga et al., 2019; Stabile et al., 2013; von Massenhausen et al., 2013; Xu et al., 2011). To date, most EGFR combination

therapies in HNSCC have not advanced clinically as currently available drugs have narrow therapeutic windows with overlapping toxicities, hence limiting the ability to safely deliver efficacious doses of either agent. However, therapeutic synergy may allow lower doses of each individual agent, improved patient tolerability, and clinical advancement.

Here, we chose to implement a genetics-based strategy to knockout *EGFR* using CRISPR/Cas9 in an EGFR-driven model as an alternative approach to identifying the cell signaling mechanisms that compensate for loss of EGFR. We then leveraged this model to characterize: (1) the molecular consequences of *EGFR* knockout, and (2) the effective small molecular combination therapies that could block proliferation of the knockout model. Our hope is that this work could serve as a primer for leveraging complete knockouts to understand compensatory signaling mechanisms in HNSCC models.

Materials and Methods

Ethics Statement

Human subjects were not used in this study. Next generation sequencing of genomic DNA from previously established patient-derived cell lines (UM-SCC-92 and UM-SCC-104) was covered under an IRB protocol approved by the University of Michigan ethics board.

Cell Culture

UM-SCC-92 wildtype, UM-SCC-92 *EGFR* knockout and UM-SCC-104 cell lines were cultured at 37°C in Dulbecco's Modified Eagle's Medium (DMEM) (Catalog No: 11965; Invitrogen, Carlsbad, CA) with 10% fetal bovine serum (FBS), 1% non-essential amino acids (NEAA) (Catalog No: 15140122; Invitrogen, Carlsbad, CA) and 7 μL/mL penicillin-streptomycin (Catalog No: 15140122; Invitrogen, Carlsbad, CA) in a humidified atmosphere with 5% CO_2. We used genotyping to confirm authenticity and tested for contamination from mycoplasma using the MycoAlert detection kit (Lonza, Basel, Switzerland). Details of DNA copy number analysis were described in a previous publication (Ludwig et al., 2018). The *EGFR* status of UM-SCC-92 wildtype cells was confirmed with previously reported Nimblegen V2 exome capture-based experiments (Liu et al., 2013).

Genomic DNA Purification

Cells were washed in PBS, and the pellet frozen at −20°C. After thawing, the pellet was re-suspended in 700 μL of Nuclei Lysis Solution (Promega, Madison, WI) and heated to 55°C for one hour. 200 μL of Protein Precipitation Solution (Promega) was added, and the solution was mixed and placed on ice for at least five minutes. After centrifuging at 13,000 RPM and 4°C for five minutes, the supernatant was transferred to a tube containing 600 μL of isopropanol. Another centrifugation (13,000 RPM for one minute) was performed and the supernatant was aspirated. Finally, the DNA pellet was washed in 200 μL of 70% ethanol and dried before re-suspending in 30-50 μL of nuclease-free water.

Sanger Sequencing

PCR was performed Platinum *Taq* DNA Polymerase High Fidelity (Invitrogen, Carlsbad, CA) as described (Smith et al., 2019) to amplify genomic DNA from *EGFR* K/O

cells (forward and reverse sequences 5'-GGCTTTCTGACGGGAGTCAA-3' and 5'-CTGTATTTGCCCTCGGGGTT-3', respectively). PCR products were cloned into the pCR8 vector system according to manufacturer's instructions and isolated DNA using the QIAprep spin mini-prep kit (Qiagen, Hilden, Germany). Sanger sequencing was performed at the University of Michigan DNA Sequencing Core on the 3730XL DNA Sequencer (Applied Biosystems, Foster City, CA) as described (Birkeland et al., 2017). DNASTAR Lasergene software suite was used to align the sequencing results to the wildtype *EGFR* sequence.

Chemicals

All compounds (gefitinib, BGJ398, ADW742, and BV-6) were obtained from Selleck Chemicals (Houston, TX). Compounds were initially dissolved in 100% sterile DMSO to 10 mM and were diluted in media to the indicated concentrations for *in vitro* studies.

Resazurin Assay

The Multiflo liquid handling dispensing system was used to seed 2,000 cells per well for wildtype UM-SCC-92 and 1,000 cells per well for UM-SCC-92 *EGFR* K/O (cell density was reduced due to large cell size) in 50 μL volume in 384-well microplates. The following day, cells were treated in quadruplicate with complete media containing 0.5% DMSO or inhibitor using a 10-point two-fold dilution series. To accomplish this, 96-well plates with inhibitors in 200X concentration was prepared and then diluted to 10X concentration in complete media in a second 96-well plate. For these dilutions, the Agilent (Santa Clara, CA) Bravo Automated Liquid Handling Platform and VWorks Automation Control Software was used as described previously (Michmerhuizen et al., 2019). Cells were treated with the desired compound concentration, again using liquid handling robotics. For combination with 5 μM gefitinib, 5 μL of 50 μM (10X) gefitinib in media to one of two 384 well plates treated in parallel with BGJ398 and ADW742 or BV-6 combinations.

In all cases, resazurin (Sigma, St Louis, MO) was dissolved in serum-free media to 440 μM and 10 μL was added to each well of cells for 12-24 hours prior to quantification. After 72 hour exposure, quantification was performed using the Cytation3 fluorescence plate reader with 540 nm excitation and 612 nm emission wavelengths. Prism 8 software was used to plot the data; concentration response curves were created using the log(inhibitor) vs. response -- Variable slope model with four parameters (IC_{50}, top, bottom, and Hill slope) allowed to vary.

For monotherapy experiments in UM-SCC-92 WT and *EGFR* K/O cell lines, the AUC model from GraphPad Prism 8 software was used to assess the treatment effect for each cell line and compound tested. The average value obtained from two independent experiments was used to generate the heatmap shown. Of note, viability data for BV-6/ADW742 from concentrations 0.625 μM, 1.25 μM, 2.5 μM and 5 μM are inferred from the dose-response curve after nonlinear regression by GraphPad Prism. Statistical analysis of synergism was completed using the Combenefit software under the Loewe synergy model (52).

Trypan Blue Dye Exclusion Assay

To assess growth rates in UM-SCC-92 WT and *EGFR* K/O models, 20,000 cells were seeded per well in 24-well cell culture plates. After 24, 48, 72 or 96 hours, cells were trypsinized, pelleted, and resuspended in in 50 μL of medium. 10 μL of cell suspension and 10 μL of trypan blue dye (0.4%, Invitrogen, Carlsbad, CA) were mixed. Total cell number for each well was determined by averaging two determinations using the Automated Cell Counter (Invitrogen, Carlsbad, CA). Six technical replicates were performed at each time point, and experiments were repeated independently three times.

Western Blotting

Western blot analysis was performed as previously described (Ludwig et al., 2018; Tillman et al., 2016). Briefly, 70-80% confluent cells were rinsed with PBS then lysed in RIPA buffer containing 1% NP40 as well as protease and phosphatase inhibitors (Catalog Nos: 186129, 1861277; ThermoFisher, Waltham, MA) as described (Michmerhuizen et al., 2016). Primary and secondary antibodies were purchased from Cell Signaling Technology (Danvers, MA) or Origene (Rockville, MD) and Jackson ImmunoResearch (West Grove, PA), respectively. Catalog numbers for all antibodies are given in Table S1. Images at 300 dpi or greater were digitally retained from all western blots and representative data is shown.

Exome Sequencing and Variant Analysis

Genomic DNA from UM-SCC-92 and *EGFR* K/O cell line was extracted according to Gentra PureGene Handbook (Qiagen, Hilden, Germany) and genotyped. Exome Capture Library Construction was performed using the Roche (Basel, Switzerland) NimbleGen V3, and paired-end sequencing (2x150 bp) of the captured exons was carried out on an Illumina (San Diego, CA) HiSeq 2500 High-Output at the University of Michigan DNA sequencing core according to standard protocol as described (Haring et al., 2021). Variant calling was performed as previously described. Variants reported were required to have at least 5 reads supporting the variant allele, and variants reported as intergenic or intronic were filtered out.

RNA Sequencing

RNA was isolated with the Qiagen (Hilden, Germany) RNeasy Spin Prep Kit and submitted to the University of Michigan DNA sequencing core as described (Mann et al., 2023). Sequencing libraries were prepared according to manufacturer's protocols with the Illumina (San Diego, CA) TruSeq stranded mRNA kit and sequenced by paired end sequencing on the Illumina HiSeq 2500-Rapid as previously described (Ludwig et al., 2018).

Transcriptome Quantification

Quality of the RNA sequencing reads was determined using FastQC v0.11.5 and no quality issues were identified. A two-step alignment protocol of Star v2.5.3a was used to map the reads. Genome index files were generated in the first step with the help of reference human genome and annotated transcriptome files. These index files were then used to guide read mapping in the second step. To retain only uniquely mapped reads, Samtools v1.9 and Picard v2.4.1 were used. Further, FPKM was computed using Cufflinks v2.2.1 with default parameters except for "--max-bundle-frags" which was changed to 100000000. This

modification was made to avoid raising of the HIDATA flag at loci that have more fragments than the pre-set threshold for every locus as described (Heft Neal et al., 2021). Raw FPKM values were compared for UM-SCC-92 wildtype and *EGFR* K/O cell lines.

Gene Set Enrichment Analysis

Gene set enrichment analysis was performed on all genes with FPKM > 1 using the software GSEA v4.03 from the Broad Institute (http://software.broadinstitute.org/gsea/index.jsp). We prepared the Pre-ranked gene list based on the log2-folder change and selected the gene sets used from the Molecular Signatures Database v7.0, including hallmark gene sets, motif gene sets, GO biological process gene sets, oncogenic gene sets and immunologic gene sets.

Transcript Analysis by qPCR

Cells were rinsed with PBS and then preserved in Qiazol (Qiagen, Hilden, Germany) at −80°C until RNA extraction was performed using RNeasy Spin Kit (Qiagen, Hilden, Germany) according to manufacturer recommendations. cDNA templates were then synthesized using random primers and SuperScript III Reverse Transcriptase (Invitrogen, Carlsbad, CA) as described (Mann et al., 2019). Primers used for qPCR analysis are listed in Table S2. Amplification by qPCR was performed with Quantitech Sybr Green (Qiagen, Hilden, Germany) on QuantStudio5 (Applied Biosystems, Foster City, CA) under the cycling conditions recommended by manufacturer.

Results

Generation of an EGFR Knockout Model to Study EGFR Resistance

To begin, we generated CRISPR/Cas9-mediated knockout (K/O) of *EGFR* in the patient-derived HNSCC cell line, UM-SCC-92. The UM-SCC-92 wildtype (WT) cell line has 3 copies of *EGFR* (Ludwig et al., 2018), and in our newly derived knockout cell line, all three alleles of *EGFR* contain deletions leading to deleterious frame-shifts (Figure 1A). EGFR protein expression is not detected by Western blot confirming knockout of expression (Figure 1B). Given the loss of EGFR protein expression in the knockout, we then used immunoblotting to evaluate any changes in cell signaling between UM-SCC-92 WT and *EGFR* K/O cell lines. We observed that downstream activation of effectors such as AKT and ERK1/2 were still present in the *EGFR* K/O, despite the lack of EGFR (Figure 1B).

Based on previous results from our lab and others showing that EGFR and FGFR inhibitor dual-therapy is effective in preclinical models of HNSCC (Goke et al., 2015; Koole et al., 2016; Michmerhuizen et al., 2022; von Massenhausen et al., 2013), we postulated that a complete loss of EGFR signaling may lead to reliance on FGF signaling if the FGF signaling pathway was indeed a primary compensatory pathway in a particular model. We also observed an increase in FGFR1 protein expression in the *EGFR* K/O, consistent with the upregulated *FGFR1* gene expression (Figure S1). Furthermore, MET phosphorylation or total protein expression was unchanged, again suggesting that this pathway may not be a critical mediator of EGFR signaling in UM-SCC-92. Finally, we evaluated expression of IGF-1R and XIAP based on the efficacy of EGFR and IGF-1R or XIAP inhibition in

HNSCC models (Guix et al., 2008; Jameson et al., 2011), but little change in the expression of either IGF-1R or XIAP was noted in the K/O model.

We noted that the *EGFR* K/O cell line also displays morphological differences as compared to the parental UM-SCC-92 cell line, perhaps indicative of a more mesenchymal phenotype (Figure 1C). Additionally, consistent with the known role of EGFR in cell growth and proliferation, the *EGFR* K/O cell line has a significantly slower proliferation rate than UM-SCC-92 cells with wildtype *EGFR* (Figure 1D).

Genetic and Molecular Characterization of the Knockout Model

As the *EGFR* K/O cell line, while slower growing, was capable of surviving without *EGFR*, we next wanted to interrogate the gene or pathway that might be compensating for the loss of EGFR signaling. We first postulated that a gain of function mutation might have occurred during the CRISPR/Cas9 and cloning process, which would help the *EGFR* K/O cell line survive. Exome sequencing of the *EGFR* K/O cell line identified 89 non-synonymous mutations not observed in WT UM-SCC-92 cells (Ludwig et al., 2018). The non-synonymous mutations are categorized by effect score in Table S3. Importantly, there were no gain of function mutations in notable kinases including Ras, PI3Kα, or FGF receptors. This analysis also confirmed that no wild type reads were observed in the *EGFR* knockout model across the *EGFR* gRNA target site (data not shown). We then analyzed the transcriptome of the *EGFR* K/O cell line, hypothesizing that a compensatory pathway may be upregulated in response to the loss of *EGFR*. This analysis generated a signature of 222 genes that were >2 log2-fold overexpressed and 288 genes that were >2 log-2-fold repressed in the knockout model compared to control cells, of which 23 were kinases (Table S4). We then analyzed the full rank list of genes for enriched molecular concepts with FDR < 0.05 using GSEA software. We identified one gene set that was positively correlated with our transcriptome signature, Hallmark Epithelial to Mesenchymal Transition (Figure 2A), which was consistent with the morphological changes observed in the knockout model (Figure 1C). The analysis also identified 91 gene sets that were negatively correlated with our knockout signature, including GO_Keratinization, GO_Cornification and GO_Epidermal Differentiation (Figure 2A), supporting a de-differentiation phenotype towards a basal cell phenotype of the knockout model. Indeed, further analysis of classical Epithelial to Mesenchymal Transition associated genes including *CDH1* (E Cadherin), *CDH2* (N Cadherin), *VIM* (Vimentin), *SNAI1* (Snail1), *SNAI2* (Snail2), *ZEB1* and *TWIST1* confirmed the associated biochemical changes between the *EGFR* K/O and WT cell line (Figure S1)

To then understand how *EGFR* K/O may help identify synergistic pathway targets, we analyzed the expression of gene targets of small molecules identified in our high throughput screen above. The greatest changes in expression were observed in FGFRs: there was a dramatic increase in *FGFR1* gene expression in the *EGFR* K/O cell line, and *FGFR2* and *FGFR3* were downregulated (Figure 2B). We confirmed the upregulation of *FGFR1* and downregulation of *FGFR2* that was observed in the RNAseq data by qPCR (Figure S2). *PIK3CA*, a known compensatory signaling mechanism to loss of EGFR, showed no transcriptome changes.

Sensitivity of EGFR Knockout Cells to Small Molecule Inhibitor Mono- and Di-Therapies

To further explore pathways responsible for compensatory resistance following EGFR depletion, we profiled the responses of UM-SCC-92 WT and *EGFR* K/O cells to a panel of small molecule inhibitors as monotherapies, hypothesizing that *EGFR* K/O cells would display heightened sensitivity to treatment with single agent inhibitors targeting genes or pathways co-dependent with EGFR signaling. Using resazurin cell viability assays, we surprisingly observed that responses to monotherapies were modest at best. Overall, no single agent resulted in exquisite sensitivity in the K/O model. Specific treatments were capable, however, of shifting responses toward sensitivity or resistance in each model (Figure 3A). For example, we observed that a decrease in cell viability is observed with high concentrations of gefitinib in the WT UM-SCC-92 cell line, but the *EGFR* K/O cell line does not respond to EGFR inhibition (Figure 3A). Additionally, PI3Kα/δ inhibitor pictilisib was less effective in the *EGFR* K/O cell line (Figure 3B), perhaps due to the upregulation of *PIK3CD* gene expression identified in this cell line (Figure 2B). *EGFR* K/O cells were slightly more sensitive to FGFR inhibition using BGJ398, and XIAP inhibition using BV-6 as compared the UM-SCC-92 WT model, but displayed minimal changes in sensitivity to IGF-1R inhibitor ADW742 (Figure 3C-E). Nevertheless, the majority of EGFR K/O cells were still viable following treatment with micromolar concentrations of these three inhibitors.

Based on the limited sensitivity of *EGFR* K/O cells to targeted small molecule inhibitors as monotherapies, we sought to evaluate the hypothesis that *EGFR* K/O cells would be responsive to combination therapies targeting additional compensatory signaling pathways. Thus, we examined the responses to FGFR inhibitor combinations in UM-SCC-92 WT and *EGFR* K/O cells. Our dual-therapy experiments demonstrated that the ability of BV-6 and ADW742 treatment to decrease cell viability synergistic over a much greater range of dose combinations with BGJ398 in UM-SCC-92 *EGFR* K/O cells, but not in WT cells (Figure 4A-D). This suggested, as we hypothesized, that the *EGFR* K/O clone was dependent on both FGFR and on additional pathways (including those involving IGF-1R and XIAP). Of note, dual-therapies were not universally more effective in the K/O model; BV-6 and ADW742 co-treatment displayed non-synergistic effects in both the UM-SCC-92 WT and *EGFR* K/O cell lines (Figure S3,4).

To determine if co-dependence on FGFR and either IGF-1R or XIAP was a specific effect of the lack of EGFR signaling in the K/O model, we then tested the dependence of these inhibitors on EGFR activity in the UM-SCC-92 WT cells treated with tri-therapies of gefitinib, BGJ398 and either ADW742 or BV-6 (Figure 4E, F). Here, we observed that the addition of 5 μM gefitinib (this concentration does not affect UM-SCC-92 cell viability when administered as monotherapy) to BGJ398 and ADW742 or to BGJ398 and BV-6 in WT cells further improved the effects of each dual-therapy, analogous to what was observed in the *EGFR* K/O model. Thus, the inhibition of FGFR and either IGF-1R or XIAP in the absence of EGFR signaling is more beneficial than the dual inhibition of FGFR and either IGF-1R or XIAP.

Finally, we tested if these combinations could reverse EGFR inhibitor resistance in a model with innate resistance to Cetuximab. Review of the literature for models of intrinsic

cetuximab resistance identified a series of papers that characterize UM-SCC-104, as naturally Cetuximab resistant (intrinsic resistance) (Baysal et al., 2020; De Pauw et al., 2018). We confirmed expression of each target gene in the cell line, and expression is shown relative to other HNSCC cell lines, Figure S4. Consistent with the published Cetuximab resistance data, Gefitinib did not inhibit proliferation of this model under our experimental system. Critically, the addition of FGFR and either IGF-1R or XIAP inhibitors showed little to no effect in the model in the absence of Gefitinib, but the triad of EGFR, FGFR and IGF1R inhibition induced significant synergistic loss of proliferation (Figure 5, Figure S5, Table S5). This data is consistent with the concept of multi-tyrosine kinase compensation as a mechanism of EGFR inhibitor resistance in HNSCC.

Discussion

Our UM-SCC-92 CRISPR/Cas9-mediated *EGFR* knockout cell line represents a unique and powerful model to reveal important insights about EGFR depletion in HNSCC. Frequent overexpression of EGFR in this cancer type (Grandis & Tweardy, 1993; Ozanne et al., 1986) suggests the functional importance of the EGFR signaling pathway in HNSCC, but the effects of EGFR depletion are incompletely understood due to limitations of other common model systems. For example, the contribution of EGFR to oncogenic phenotypes is difficult to assess using siRNA or shRNA due to the incomplete knockout provided by these techniques. EGFR inhibitors block only a subset of the functions of the receptor, depending on their interaction site, and leave inactive EGFR protein in the cell. *EGFR* homozygous knockout mice display strain-specific deleterious phenotypes; if viable at all, these mice do not reach three weeks of age (Sibilia & Wagner, 1995). In contrast, the UM-SCC-92 *EGFR* K/O cell line is to our knowledge the first HNSCC model with complete loss of *EGFR* and may represent the optimal model for the advancing class of EGFR-degrading molecules that are currently in development.

Characterization of our *EGFR* K/O model identified both expected and unexpected phenotypes. For example, we observed that our *EGFR* K/O cells, consistent with the role of EGFR signaling in cell proliferation, displayed blunted growth compared to WT UM-SCC-92 cells (Figure 1D). A similar finding was reported when CRISPR/Cas9 was used to knockout *EGFR* in a renal cell carcinoma cell line that overexpressed the receptor prior to genome editing (Liu et al., 2020). We also found, as expected, that *EGFR* knockout cells had reduced sensitivity to EGFR inhibitor gefitinib (Figure 3A). Additionally, even though EGFR overexpression has been implicated in cancer metastasis (Radinsky et al., 1995), characterization of our EGFR K/O model revealed a mesenchymal phenotype (Figure 1C), suggesting that mesenchymal signaling may be a critical factor in bypassing EGFR-dependence. This result included the downregulation of genes involved in keratinization and upregulation of genes necessary for epithelial to mesenchymal transition (EMT) (Figure 2A). Importantly, our data is consistent with previous data suggesting that EMT can be driver of EGFR inhibitor resistance in non-small cell lung cancer (Weng et al., 2019; Yochum et al., 2019) and HNSCC (Cardnell et al., 2013; Haddad et al., 2009).

Also consistent with previous reports is our data highlighting FGFR signaling as a possible mechanism of resistance to EGFR-targeting therapy (Goke et al., 2015; Koole et al., 2016;

von Massenhausen et al., 2013). Further, XIAP antagonists have also shown synergism with EGFR-targeting agents in HNSCC and other cancer types (Foster et al., 2009; Lee et al., 2014; Michmerhuizen et al., 2022), and while XIAP expression was unchanged in EGFR K/O cells (Figure 2B), our *EGFR* K/O cells were more sensitive than wildtype cells to treatment with XIAP inhibitor BV-6 (Figure 3E). The sensitivity of K/O cells to combined FGFR and IGF-1R or XIAP inhibition (Figure 4) suggests that UM-SCC-92 cells are dependent on multiple signaling pathways, including not only EGFR and FGFR, but also IGF-1R and/or XIAP. This result has at least two important implications with the potential to improve targeted therapy regimens for HNSCC. First, these data and others demonstrate synergistic effects of a XIAP inhibitor and FGFR inhibitor following short- or long-term EGFR depletion which suggests incorporation of IAP inhibitors may facilitate clinically tolerable combinations of EGFR and FGFR inhibitors. Combinations of EGFR and FGFR inhibitors are associated with dose-limiting toxicities both *in vivo* and in clinical trials (Das et al., 2015); however XIAP inhibition could allow EGFR- and FGFR-targeting therapies to be used in lower, safer quantities. A recent study in HNSCC has shown administration of an IAP inhibitor with concurrent chemoradiation results in significantly improved outcomes compared to chemoradiation alone without a significant increase in toxicities (Sun et al., 2020). These results support the potential role of IAP inhibition as a synergistic approach in HNSCC. Second, given the lack of clinical response following EGFR and IGF-1R inhibitors in clinical studies to date, our findings suggest that signaling through FGFR or even other RTKs may be responsible for resistance to EGFR and IGF-1R dual-therapy and motivate additional exploration of this hypothesis in preclinical models. As such, understanding how to effectively treat tumors with rapid multi-kinase compensation as we observed in this model system remains an important area of investigation in our field, and recent data has novel agents that may prove better tolerated in EGFR inhibitor combinations (Jin et al., 2021).

In summary, we present here a novel model of total, long-term depletion of *EGFR* in HNSCC. Through our investigation of the consequences of *EGFR* knockout on cell gene expression and drug response, we reveal possible compensatory mechanisms that might be leveraged in future studies to overcome resistance to EGFR inhibition and provide additional targeted therapy regimens that offer a survival benefit in HNSCC.

Supplementary Material

Refer to Web version on PubMed Central for supplementary material.

Acknowledgments

This work was supported by the National Institutes of Health National Institute of Dental and Cranofacial Research (Grant U01-DE025184), the National Science Foundation (Grant DGE-1256260), and funds from the American Head and Neck Society. NLM received support from a National Science Foundation Graduate Research Fellowship DGE-1256260, and MLL was supported by F31 CA206341-03 from the National Institutes of Health National Institute of Dental and Cranofacial Research.

Abbreviations:

DMEM	Dulbecco’s Modified Eagle’s Medium

DMSO	dimethyl sulfoxide
DNMT	DNA methyl transferase
EGFR	epidermal growth factor receptor
FBS	fetal bovine serum
FGFR	fibroblast growth factor receptor
HNSCC	head and neck squamous cell carcinoma
IC_{50}	half-maximal inhibitory concentration
IGFR	insulin-like growth factor receptor
MEV	multiple experiment viewer
PI3K	phosphatidylinositol 3-kinase
XIAP	X-linked inhibitor of apoptosis

References

Anisuzzaman AS, Haque A, Wang D, Rahman MA, Zhang C, Chen Z, Chen ZG, Shin DM, & Amin AR (2017). In Vitro and In Vivo Synergistic Antitumor Activity of the Combination of BKM120 and Erlotinib in Head and Neck Cancer: Mechanism of Apoptosis and Resistance. Mol Cancer Ther, 16(4), 729–738. 10.1158/1535-7163.Mct-16-0683 [PubMed: 28119490]

Baysal H, De Pauw I, Zaryouh H, De Waele J, Peeters M, Pauwels P, Vermorken JB, Smits E, Lardon F, Jacobs J, & Wouters A (2020). Cetuximab-induced natural killer cell cytotoxicity in head and neck squamous cell carcinoma cell lines: investigation of the role of cetuximab sensitivity and HPV status. Br J Cancer, 123(5), 752–761. 10.1038/s41416-020-0934-3 [PubMed: 32541873]

Birkeland AC, Foltin SK, Michmerhuizen NL, Hoesli RC, Rosko AJ, Byrd S, Yanik M, Nor JE, Bradford CR, Prince ME, Carey TE, McHugh JB, Spector ME, & Brenner JC (2017). Correlation of Crtc1/3-Maml2 fusion status, grade and survival in mucoepidermoid carcinoma. Oral Oncology, 68, 5–8. 10.1016/j.oraloncology.2017.02.025 [PubMed: 28438292]

Brondum L, Alsner J, Sorensen BS, Maare C, Johansen J, Primdahl H, Evensen JF, Kristensen CA, Andersen LJ, Overgaard J, & Eriksen JG (2018). Associations between skin rash, treatment outcome, and single nucleotide polymorphisms in head and neck cancer patients receiving the EGFR-inhibitor zalutumumab: results from the DAHANCA 19 trial. Acta Oncol, 57(9), 1159–1164. 10.1080/0284186X.2018.1464664 [PubMed: 29771169]

Burtness B, Haddad R, Dinis J, Trigo J, Yokota T, de Souza Viana L, Romanov I, Vermorken J, Bourhis J, Tahara M, Martins Segalla JG, Psyrri A, Vasilevskaya I, Nangia CS, Chaves-Conde M, Kiyota N, Homma A, Holeckova P, Del Campo JM, Asarawala N, Nicolau UR, Rauch D, Even C, Wang B, Gibson N, Ehrnrooth E, Harrington K, Cohen EEW, Head LUX, & Neck i. (2019). Afatinib vs Placebo as Adjuvant Therapy After Chemoradiotherapy in Squamous Cell Carcinoma of the Head and Neck: A Randomized Clinical Trial. JAMA Oncol, 5(8), 1170–1180. 10.1001/jamaoncol.2019.1146 [PubMed: 31194247]

Burtness B, Harrington KJ, Greil R, Soulieres D, Tahara M, de Castro G Jr., Psyrri A, Baste N, Neupane P, Bratland A, Fuereder T, Hughes BGM, Mesia R, Ngamphaiboon N, Rordorf T, Wan Ishak WZ, Hong RL, Gonzalez Mendoza R, Roy A, Zhang Y, Gumuscu B, Cheng JD, Jin F, Rischin D, & Investigators K.-. (2019). Pembrolizumab alone or with chemotherapy versus cetuximab with chemotherapy for recurrent or metastatic squamous cell carcinoma of the head and neck (KEYNOTE-048): a randomised, open-label, phase 3 study. Lancet, 394(10212), 1915–1928. 10.1016/S0140-6736(19)32591-7 [PubMed: 31679945]

Cancer Genome Atlas N. (2015). Comprehensive genomic characterization of head and neck squamous cell carcinomas. Nature, 517(7536), 576–582. 10.1038/nature14129 [PubMed: 25631445]

Cardnell R, Diao L, Wang J, Bearss D, Warner S, Fan YH, Giri U, Story MD, Weinstein JN, Coombes KR, Williams MD, Network TCGAR, Wistuba II, Mills GB, Myers J, William WN, Ang KK, Heymach J, & Byers LA (2013). An epithelial-mesenchymal transition (EMT) gene signature to predict resistance to EGFR inhibition and AXL identification as a therapeutic target in head and neck squamous cell carcinoma. 31(15_suppl), 6011–6011. 10.1200/jco.2013.31.15_suppl.6011

D'Amato V, Rosa R, D'Amato C, Formisano L, Marciano R, Nappi L, Raimondo L, Di Mauro C, Servetto A, Fusciello C, Veneziani BM, De Placido S, & Bianco R (2014). The dual PI3K/mTOR inhibitor PKI-587 enhances sensitivity to cetuximab in EGFR-resistant human head and neck cancer models. Br J Cancer, 110(12), 2887–2895. 10.1038/bjc.2014.241 [PubMed: 24823695]

Das M, Padda SK, Frymoyer A, Zhou L, Riess JW, Neal JW, & Wakelee HA (2015). Dovitinib and erlotinib in patients with metastatic non-small cell lung cancer: A drug-drug interaction. Lung Cancer, 89(3), 280–286. 10.1016/j.lungcan.2015.06.011 [PubMed: 26149476]

De Pauw I, Lardon F, Van den Bossche J, Baysal H, Fransen E, Deschoolmeester V, Pauwels P, Peeters M, Vermorken JB, & Wouters A (2018). Simultaneous targeting of EGFR, HER2, and HER4 by afatinib overcomes intrinsic and acquired cetuximab resistance in head and neck squamous cell carcinoma cell lines. Mol Oncol, 12(6), 830–854. 10.1002/1878-0261.12197 [PubMed: 29603584]

Di Veroli GY, Fornari C, Wang D, Mollard S, Bramhall JL, Richards FM, & Jodrell DI (2016). Combenefit: an interactive platform for the analysis and visualization of drug combinations. Bioinformatics, 32(18), 2866–2868. 10.1093/bioinformatics/btw230 [PubMed: 27153664]

Dieci MV, Arnedos M, Andre F, & Soria JC (2013). Fibroblast growth factor receptor inhibitors as a cancer treatment: from a biologic rationale to medical perspectives. Cancer Discov, 3(3), 264–279. 10.1158/2159-8290.Cd-12-0362 [PubMed: 23418312]

Foster FM, Owens TW, Tanianis-Hughes J, Clarke RB, Brennan K, Bundred NJ, & Streuli CH (2009). Targeting inhibitor of apoptosis proteins in combination with ErbB antagonists in breast cancer. Breast Cancer Res, 11(3), R41. 10.1186/bcr2328 [PubMed: 19563669]

Goke F, Franzen A, Hinz TK, Marek LA, Yoon P, Sharma R, Bode M, von Maessenhausen A, Lankat-Buttgereit B, Goke A, Golletz C, Kirsten R, Boehm D, Vogel W, Kleczko EK, Eagles JR, Hirsch FR, Van Bremen T, Bootz F, Schroeck A, Kim J, Tan AC, Jimeno A, Heasley LE, & Perner S (2015). FGFR1 Expression Levels Predict BGJ398 Sensitivity of FGFR1-Dependent Head and Neck Squamous Cell Cancers. Clin Cancer Res, 21(19), 4356–4364. 10.1158/1078-0432.CCR-14-3357 [PubMed: 26015511]

Grandis JR, & Tweardy DJ (1993). Elevated levels of transforming growth factor alpha and epidermal growth factor receptor messenger RNA are early markers of carcinogenesis in head and neck cancer. Cancer Res, 53(15), 3579–3584. [PubMed: 8339264]

Guix M, Faber AC, Wang SE, Olivares MG, Song Y, Qu S, Rinehart C, Seidel B, Yee D, Arteaga CL, & Engelman JA (2008). Acquired resistance to EGFR tyrosine kinase inhibitors in cancer cells is mediated by loss of IGF-binding proteins. J Clin Invest, 118(7), 2609–2619. 10.1172/jci34588 [PubMed: 18568074]

Haddad Y, Choi W, & McConkey DJ (2009). Delta-crystallin enhancer binding factor 1 controls the epithelial to mesenchymal transition phenotype and resistance to the epidermal growth factor receptor inhibitor erlotinib in human head and neck squamous cell carcinoma lines. Clin Cancer Res, 15(2), 532–542. 10.1158/1078-0432.CCR-08-1733 [PubMed: 19147758]

Haring CT, Bhambhani C, Brummel C, Jewell B, Bellile E, Heft Neal ME, Sandford E, Spengler RM, Bhangale A, Spector ME, McHugh J, Prince ME, Mierzwa M, Worden FP, Tewari M, Swiecicki PL, & Brenner JC (2021). Human papilloma virus circulating tumor DNA assay predicts treatment response in recurrent/metastatic head and neck squamous cell carcinoma. Oncotarget, 12(13), 1214–1229. 10.18632/oncotarget.27992 [PubMed: 34194620]

Hartmann S, Bhola NE, & Grandis JR (2016). HGF/Met Signaling in Head and Neck Cancer: Impact on the Tumor Microenvironment. Clin Cancer Res, 22(16), 4005–4013. 10.1158/1078-0432.CCR-16-0951 [PubMed: 27370607]

Heft Neal ME, Gensterblum-Miller E, Bhangale AD, Kulkarni A, Zhai J, Smith J, Brummel C, Foltin SK, Thomas D, Jiang H, McHugh JB, & Brenner JC (2021). Integrative sequencing discovers

an ATF1-motif enriched molecular signature that differentiates hyalinizing clear cell carcinoma from mucoepidemoid carcinoma. Oral Oncol, 117, 105270. 10.1016/j.oraloncology.2021.105270 [PubMed: 33827033]

Jameson MJ, Beckler AD, Taniguchi LE, Allak A, Vanwagner LB, Lee NG, Thomsen WC, Hubbard MA, & Thomas CY (2011). Activation of the insulin-like growth factor-1 receptor induces resistance to epidermal growth factor receptor antagonism in head and neck squamous carcinoma cells. Mol Cancer Ther, 10(11), 2124–2134. 10.1158/1535-7163.Mct-11-0294 [PubMed: 21878657]

Jin H, Shi Y, Lv Y, Yuan S, Ramirez CFA, Lieftink C, Wang L, Wang S, Wang C, Dias MH, Jochems F, Yang Y, Bosma A, Hijmans EM, de Groot MHP, Vegna S, Cui D, Zhou Y, Ling J, Wang H, Guo Y, Zheng X, Isima N, Wu H, Sun C, Beijersbergen RL, Akkari L, Zhou W, Zhai B, Qin W, & Bernards R (2021). EGFR activation limits the response of liver cancer to lenvatinib. Nature, 595(7869), 730–734. 10.1038/s41586-021-03741-7 [PubMed: 34290403]

Koole K, Brunen D, van Kempen PM, Noorlag R, de Bree R, Lieftink C, van Es RJ, Bernards R, & Willems SM (2016). FGFR1 Is a Potential Prognostic Biomarker and Therapeutic Target in Head and Neck Squamous Cell Carcinoma. Clin Cancer Res, 22(15), 3884–3893. 10.1158/1078-0432.CCR-15-1874 [PubMed: 26936917]

Lattanzio L, Tonissi F, Monteverde M, Vivenza D, Russi E, Milano G, Merlano M, & Lo Nigro C (2015). Treatment effect of buparlisib, cetuximab and irradiation in wild-type or PI3KCA-mutated head and neck cancer cell lines. Invest New Drugs, 33(2), 310–320. 10.1007/s10637-015-0210-1 [PubMed: 25603975]

Lee SH, Lee JY, Jung CL, Bae IH, Suh KH, Ahn YG, Jin DH, Kim TW, Suh YA, & Jang SJ (2014). A novel antagonist to the inhibitors of apoptosis (IAPs) potentiates cell death in EGFR-overexpressing non-small-cell lung cancer cells. Cell Death Dis, 5, e1477. 10.1038/cddis.2014.447 [PubMed: 25321484]

Leemans CR, Braakhuis BJ, & Brakenhoff RH (2011). The molecular biology of head and neck cancer. Nat Rev Cancer, 11(1), 9–22. 10.1038/nrc2982 [PubMed: 21160525]

Liu B, Diaz Arguello OA, Chen D, Chen S, Saber A, & Haisma HJ (2020). CRISPR-mediated ablation of overexpressed EGFR in combination with sunitinib significantly suppresses renal cell carcinoma proliferation. PLoS One, 15(5), e0232985. 10.1371/journal.pone.0232985 [PubMed: 32413049]

Liu J, Pan S, Hsieh MH, Ng N, Sun F, Wang T, Kasibhatla S, Schuller AG, Li AG, Cheng D, Li J, Tompkins C, Pferdekamper A, Steffy A, Cheng J, Kowal C, Phung V, Guo G, Wang Y, Graham MP, Flynn S, Brenner JC, Li C, Villarroel MC, Schultz PG, Wu X, McNamara P, Sellers WR, Petruzzelli L, Boral AL, Seidel HM, McLaughlin ME, Che J, Carey TE, Vanasse G, & Harris JL (2013). Targeting Wnt-driven cancer through the inhibition of Porcupine by LGK974. Proc Natl Acad Sci U S A, 110(50), 20224–20229. 10.1073/pnas.1314239110 [PubMed: 24277854]

Ludwig ML, Kulkarni A, Birkeland AC, Michmerhuizen NL, Foltin SK, Mann JE, Hoesli RC, Devenport SN, Jewell BM, Shuman AG, Spector ME, Carey TE, Jiang H, & Brenner JC (2018). The genomic landscape of UM-SCC oral cavity squamous cell carcinoma cell lines. Oral Oncol, 87, 144–151. 10.1016/j.oraloncology.2018.10.031 [PubMed: 30527230]

Mann JE, Kulkarni A, Birkeland AC, Kafelghazal J, Eisenberg J, Jewell BM, Ludwig ML, Spector ME, Jiang H, Carey TE, & Brenner JC (2019). The molecular landscape of the University of Michigan laryngeal squamous cell carcinoma cell line panel. Head Neck. 10.1002/hed.25803

Mann JE, Smith JD, Kulkarni A, Foltin SK, Scheftz EB, Murray IR, Gensterblum-Miller E, Brummel CV, Bhangale A, Hoesli RC, & Brenner JC (2023). Genome-wide open reading frame profiling identifies fibroblast growth factor signaling as a driver of PD-L1 expression in head and neck squamous cell carcinoma. Oral Oncol, 146, 106562. 10.1016/j.oraloncology.2023.106562 [PubMed: 37666053]

Michmerhuizen NL, Leonard E, Kulkarni A, & Brenner JC (2016). Differential compensation mechanisms define resistance to PI3K inhibitors in PIK3CA amplified HNSCC. Otorhinolaryngol Head Neck Surg, 1(2), 44–50. https://www.ncbi.nlm.nih.gov/pubmed/28004037 [PubMed: 28004037]

Michmerhuizen NL, Leonard E, Matovina C, Harris M, Herbst G, Kulkarni A, Zhai J, Jiang H, Carey TE, & Brenner JC (2019). Rationale for Using Irreversible Epidermal Growth Factor Receptor

Inhibitors in Combination with Phosphatidylinositol 3-Kinase Inhibitors for Advanced Head and Neck Squamous Cell Carcinoma. Mol Pharmacol, 95(5), 528–536. 10.1124/mol.118.115162 [PubMed: 30858165]

Michmerhuizen NL, Ludwig ML, Birkeland AC, Nimmagadda S, Zhai J, Wang J, Jewell BM, Genouw D, Remer L, Kim D, Foltin SK, Bhangale A, Kulkarni A, Bradford CR, Swiecicki PL, Carey TE, Jiang H, & Brenner JC (2022). Small molecule profiling to define synergistic EGFR inhibitor combinations in head and neck squamous cell carcinoma. Head Neck. 10.1002/hed.27018

Okuyama K, Naruse T, & Yanamoto S (2023). Tumor microenvironmental modification by the current target therapy for head and neck squamous cell carcinoma. J Exp Clin Cancer Res, 42(1), 114. 10.1186/s13046-023-02691-4 [PubMed: 37143088]

Ozanne B, Richards CS, Hendler F, Burns D, & Gusterson B (1986). Over-expression of the EGF receptor is a hallmark of squamous cell carcinomas. J Pathol, 149(1), 9–14. 10.1002/path.1711490104 [PubMed: 2425067]

Quintanal-Villalonga A, Molina-Pinelo S, Cirauqui C, Ojeda-Márquez L, Marrugal Á, Suarez R, Conde E, Ponce-Aix S, Enguita AB, Carnero A, Ferrer I, & Paz-Ares L (2019). FGFR1 Cooperates with EGFR in Lung Cancer Oncogenesis, and Their Combined Inhibition Shows Improved Efficacy. Journal of Thoracic Oncology, 14(4), 641–655. https://doi.org/10.1016/j.jtho.2018.12.021 [PubMed: 30639621]

Radinsky R, Risin S, Fan D, Dong Z, Bielenberg D, Bucana CD, & Fidler IJ (1995). Level and function of epidermal growth factor receptor predict the metastatic potential of human colon carcinoma cells. Clin Cancer Res, 1(1), 19–31. https://www.ncbi.nlm.nih.gov/pubmed/9815883 [PubMed: 9815883]

Raj S, Kesari KK, Kumar A, Rathi B, Sharma A, Gupta PK, Jha SK, Jha NK, Slama P, Roychoudhury S, & Kumar D (2022). Molecular mechanism(s) of regulation(s) of c-MET/HGF signaling in head and neck cancer. Mol Cancer, 21(1), 31. 10.1186/s12943-022-01503-1 [PubMed: 35081970]

Rebucci M, Peixoto P, Dewitte A, Wattez N, De Nuncques MA, Rezvoy N, Vautravers-Dewas C, Buisine MP, Guerin E, Peyrat JP, Lartigau E, & Lansiaux A (2011). Mechanisms underlying resistance to cetuximab in the HNSCC cell line: role of AKT inhibition in bypassing this resistance. Int J Oncol, 38(1), 189–200. [PubMed: 21109940]

Siano M, Molinari F, Martin V, Mach N, Fruh M, Freguia S, Corradino I, Ghielmini M, Frattini M, & Espeli V (2017). Multicenter Phase II Study of Panitumumab in Platinum Pretreated, Advanced Head and Neck Squamous Cell Cancer. Oncologist, 22(7), 782–e770. 10.1634/theoncologist.2017-0069 [PubMed: 28592616]

Sibilia M, & Wagner EF (1995). Strain-dependent epithelial defects in mice lacking the EGF receptor. Science, 269(5221), 234–238. 10.1126/science.7618085 [PubMed: 7618085]

Silva-Oliveira RJ, Melendez M, Martinho O, Zanon MF, de Souza Viana L, Carvalho AL, & Reis RM (2017). AKT can modulate the in vitro response of HNSCC cells to irreversible EGFR inhibitors. Oncotarget, 8(32), 53288–53301. 10.18632/oncotarget.18395 [PubMed: 28881811]

Siu LL, Soulieres D, Chen EX, Pond GR, Chin SF, Francis P, Harvey L, Klein M, Zhang W, Dancey J, Eisenhauer EA, Winquist E, Princess Margaret Hospital Phase, I. I. C., & National Cancer Institute of Canada Clinical Trials Group, S. (2007). Phase I/II trial of erlotinib and cisplatin in patients with recurrent or metastatic squamous cell carcinoma of the head and neck: a Princess Margaret Hospital phase II consortium and National Cancer Institute of Canada Clinical Trials Group Study. J Clin Oncol, 25(16), 2178–2183. 10.1200/JCO.2006.07.6547 [PubMed: 17538162]

Smith JD, Birkeland AC, Rosko AJ, Hoesli RC, Foltin SK, Swiecicki P, Mierzwa M, Chinn SB, Shuman AG, Malloy KM, Casper KA, McLean SA, Wolf GT, Bradford CR, Prince ME, Brenner JC, & Spector ME (2019). Mutational profiles of persistent/recurrent laryngeal squamous cell carcinoma. Head Neck, 41(2), 423–428. 10.1002/hed.25444 [PubMed: 30548484]

Smith JD, Ludwig ML, Bhangale AD, Brummel C, Swiecicki PL, Worden FP, Chinn SB, Stucken CL, Rosko AJ, Prince MEP, Malloy KM, Casper KA, Bradford CR, Chepeha DB, Shah J, Schonewolf CA, McHugh JB, Nyati MK, Eisbruch A, Mierzwa ML, Spector ME, & Brenner JC (2023). Tumor immune microenvironment alterations using induction cetuximab in a phase II trial of deintensified therapy for p16-positive oropharynx cancer. Head Neck, 45(5), 1281–1287. 10.1002/hed.27344 [PubMed: 36932871]

Stabile LP, He G, Lui VW, Thomas S, Henry C, Gubish CT, Joyce S, Quesnelle KM, Siegfried JM, & Grandis JR (2013). c-Src activation mediates erlotinib resistance in head and neck cancer by stimulating c-Met. Clin Cancer Res, 19(2), 380–392. 10.1158/1078-0432.Ccr-12-1555 [PubMed: 23213056]

Sun XS, Tao Y, Le Tourneau C, Pointreau Y, Sire C, Kaminsky MC, Coutte A, Alfonsi M, Boisselier P, Martin L, Miroir J, Ramee JF, Delord JP, Clatot F, Rolland F, Villa J, Magne N, Elicin O, Gherga E, Nguyen F, Lafond C, Bera G, Calugaru V, Geoffrois L, Chauffert B, Zubel A, Zanna C, Brienza S, Crompton P, Rouits E, Gollmer K, Szyldergemajn S, & Bourhis J (2020). Debio 1143 and high-dose cisplatin chemoradiotherapy in high-risk locoregionally advanced squamous cell carcinoma of the head and neck: a double-blind, multicentre, randomised, phase 2 study. Lancet Oncol, 21(9), 1173–1187. 10.1016/S1470-2045(20)30327-2 [PubMed: 32758455]

Tillman BN, Yanik M, Birkeland AC, Liu CJ, Hovelson DH, Cani AK, Palanisamy N, Carskadon S, Carey TE, Bradford CR, Tomlins SA, McHugh JB, Spector ME, & Brenner J (2016). Fibroblast growth factor family aberrations as a putative driver of head and neck squamous cell carcinoma in an epidemiologically low-risk patient as defined by targeted sequencing. Head Neck, 38 Suppl 1, E1646–1652. 10.1002/hed.24292 [PubMed: 26849095]

Vermorken JB, Mesia R, Rivera F, Remenar E, Kawecki A, Rottey S, Erfan J, Zabolotnyy D, Kienzer HR, Cupissol D, Peyrade F, Benasso M, Vynnychenko I, De Raucourt D, Bokemeyer C, Schueler A, Amellal N, & Hitt R (2008). Platinum-based chemotherapy plus cetuximab in head and neck cancer. N Engl J Med, 359(11), 1116–1127. 10.1056/NEJMoa0802656 [PubMed: 18784101]

Vermorken JB, Trigo J, Hitt R, Koralewski P, Diaz-Rubio E, Rolland F, Knecht R, Amellal N, Schueler A, & Baselga J (2007). Open-label, uncontrolled, multicenter phase II study to evaluate the efficacy and toxicity of cetuximab as a single agent in patients with recurrent and/or metastatic squamous cell carcinoma of the head and neck who failed to respond to platinum-based therapy. J Clin Oncol, 25(16), 2171–2177. 10.1200/JCO.2006.06.7447 [PubMed: 17538161]

von Massenhausen A, Franzen A, Heasley L, & Perner S (2013). FGFR1 as a novel prognostic and predictive biomarker in squamous cell cancers of the lung and the head and neck area. Ann Transl Med, 1(3), 23. 10.3978/j.issn.2305-5839.2013.06.08 [PubMed: 25332967]

Wang J, Al-Majid D, Brenner JC, & Smith JD (2023). Mutant HRas Signaling and Rationale for Use of Farnesyltransferase Inhibitors in Head and Neck Squamous Cell Carcinoma. Target Oncol. 10.1007/s11523-023-00993-3

Weng CH, Chen LY, Lin YC, Shih JY, Lin YC, Tseng RY, Chiu AC, Yeh YH, Liu C, Lin YT, Fang JM, & Chen CC (2019). Epithelial-mesenchymal transition (EMT) beyond EGFR mutations per se is a common mechanism for acquired resistance to EGFR TKI. Oncogene, 38(4), 455–468. 10.1038/s41388-018-0454-2 [PubMed: 30111817]

Xu H, Stabile LP, Gubish CT, Gooding WE, Grandis JR, & Siegfried JM (2011). Dual blockade of EGFR and c-Met abrogates redundant signaling and proliferation in head and neck carcinoma cells. Clin Cancer Res, 17(13), 4425–4438. 10.1158/1078-0432.Ccr-10-3339 [PubMed: 21622718]

Yochum ZA, Cades J, Wang H, Chatterjee S, Simons BW, O'Brien JP, Khetarpal SK, Lemtiri-Chlieh G, Myers KV, Huang EH, Rudin CM, Tran PT, & Burns TF (2019). Targeting the EMT transcription factor TWIST1 overcomes resistance to EGFR inhibitors in EGFR-mutant non-small-cell lung cancer. Oncogene, 38(5), 656–670. 10.1038/s41388-018-0482-y [PubMed: 30171258]

Young NR, Liu J, Pierce C, Wei TF, Grushko T, Olopade OI, Liu W, Shen C, Seiwert TY, & Cohen EE (2013). Molecular phenotype predicts sensitivity of squamous cell carcinoma of the head and neck to epidermal growth factor receptor inhibition. Mol Oncol, 7(3), 359–368. 10.1016/j.molonc.2012.11.001 [PubMed: 23200321]

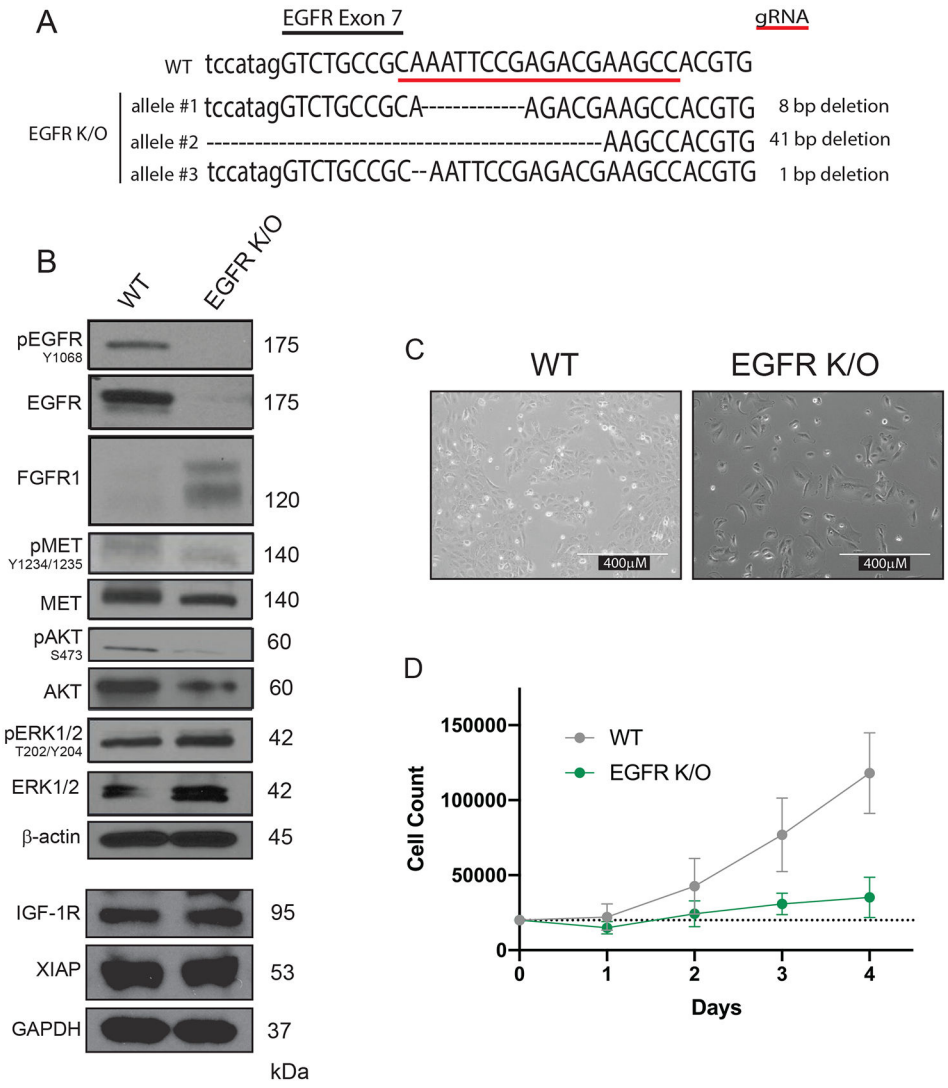

Figure 1. Generation and Characterization of UM-SCC-92 *EGFR* K/O Cells.

(**A**) Sanger sequencing was performed to confirm EGFR knockout in UM-SCC-92 cells. (**B**) Western blot analysis of phosphorylated and total EGFR, MET, AKT, and ERK expression or of total FGFR1, IGF-1R, XIAP in UM-SCC-92 WT and *EGFR* K/O cells. β-actin and GAPDH were used as loading controls. Experiments were performed in at least duplicate, and representative images are shown. (**C**) Representative images of UM-SCC-92 WT and *EGFR* K/O cells taken at 40X on Nikon Eclipse TS100. Scale bar (400 μm) is shown. (**D**) Total cell number for UM-SCC-92 WT and *EGFR* K/O cells following 24, 48, 72, or 96 hours of growth.

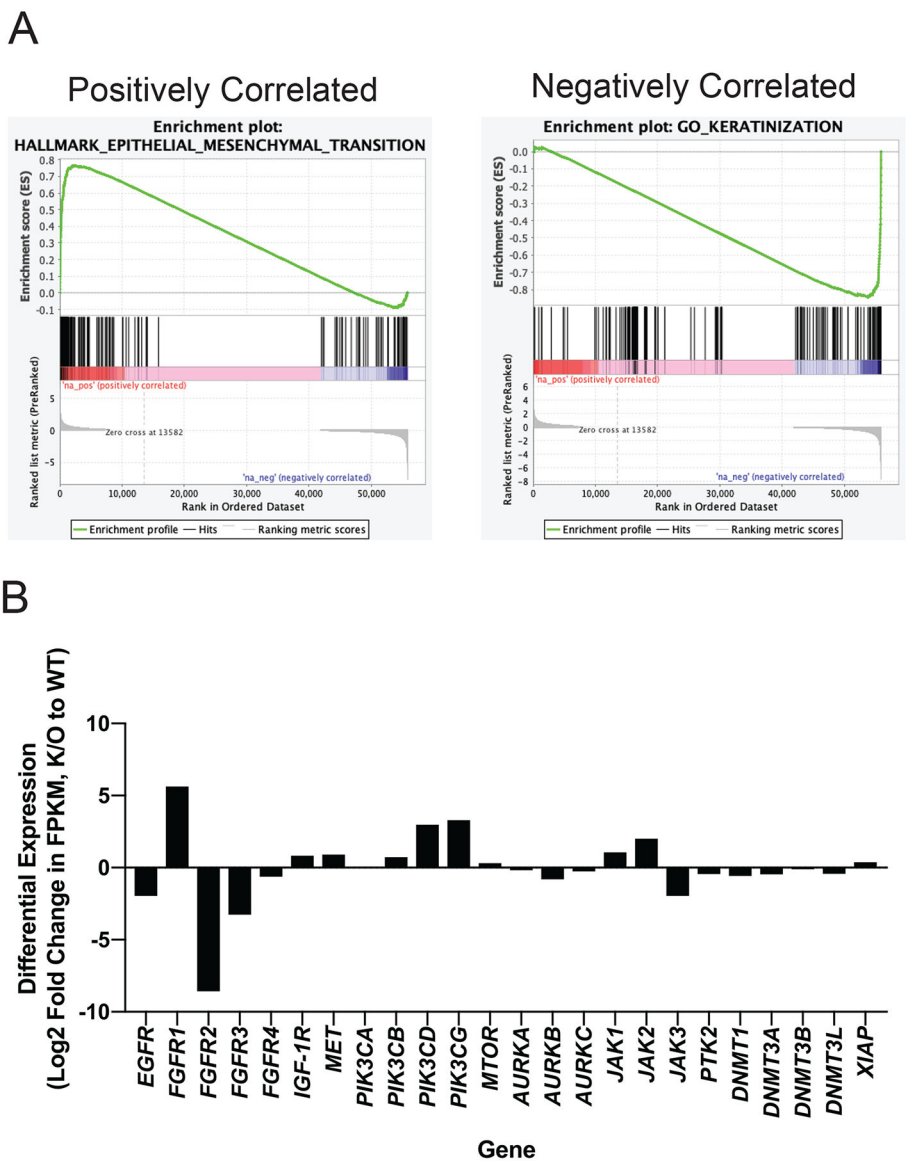

Figure 2. Transcriptional analysis of UM-SCC-92 *EGFR* K/O Cells identifies a mesenchymal gene signature, with multiple upregulated kinases.

RNA sequencing was performed for UM-SCC-92 WT and *EGFR* K/O cells, followed by identification of individual genes with significantly higher or lower expression levels in *EGFR* K/O cells and gene set enrichment analysis. (**A**) Enrichment plots show that the Hallmark epithelial to mesenchymal transition gene set and GO keratinization gene set were significantly up- and downregulated, respectively, in *EGFR* K/O cells. (**B**) Differential gene expression (log2 fold change of UM-SCC-92 *EGFR* K/O compared to WT) for top-scoring and/or validated targets from small molecule profiling.

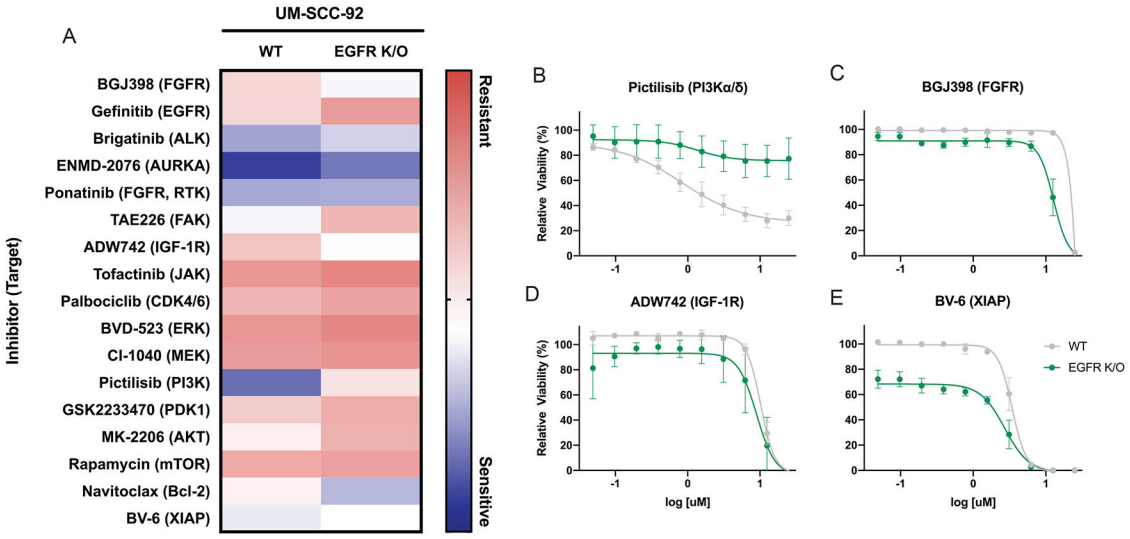

Figure 3. Effects of Monotherapy Treatment in UM-SCC-92 WT and *EGFR* K/O Cells.

(**A**) UM-SCC-92 WT and *EGFR* K/O cells were treated with increasing concentrations of the targeted small molecule inhibitors shown for 72 hours. Cell viability was measured using a resazurin cell viability assay, and the average area under the curve was calculated using the mean and s.d. of quadruplicate determinations from at least two independent experiments. Representative data (mean and s.d. of quadruplicate determinations from a single independent experiment) is shown for (**B**) PI3K α/δ inhibitor pictilisib, (**C**) FGFR inhibitor BGJ398, (**D**) IGF-1R inhibitor ADW742, and (**E**) XIAP inhibitor BV-6.

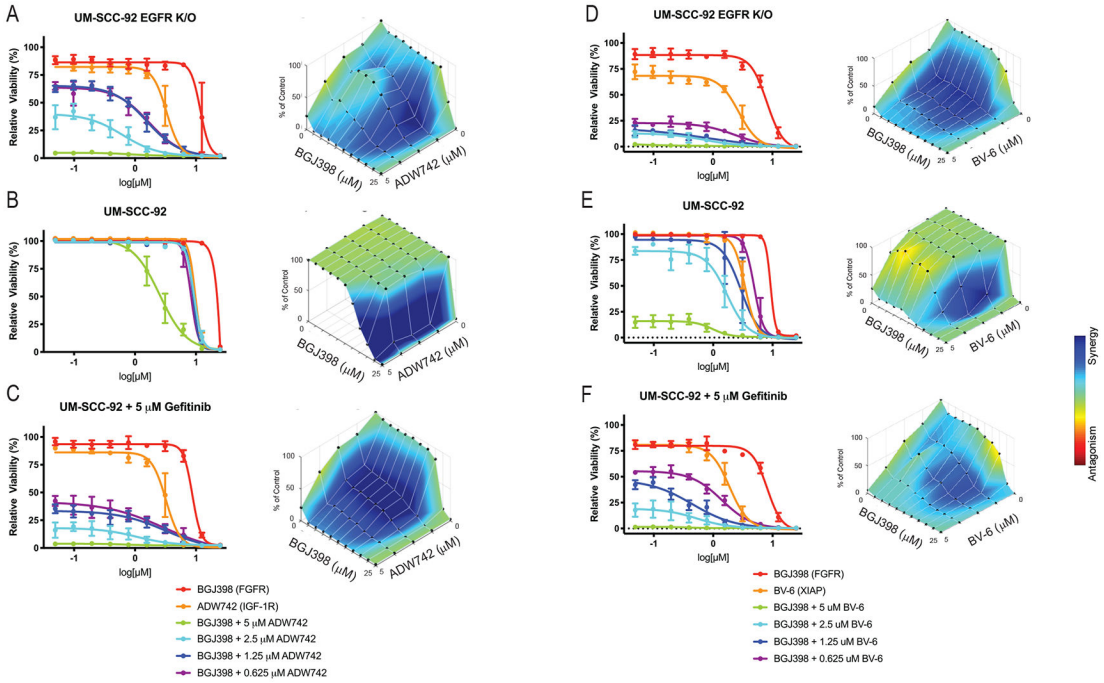

Figure 4. Effects of Combination Therapy Treatment in UM-SCC-92 WT and *EGFR* K/O Cells.

UM-SCC-92 *EGFR* K/O cells were treated with increasing concentrations of FGFR inhibitor BGJ398 and/or IGF-1R inhibitor ADW742 (**A**) or XIAP inhibitor BV-6 (**B**) for 72 hours. UM-SCC-92 WT cells were treated similarly in the absence (**C**, **D**) or presence (**E**, **F**) of 5 μM gefitinib. Cell viability was measured using a resazurin cell viability assay. Each point is the mean and s.d. of quadruplicate determinations from a single experiment. Each experiment was repeated independently at least twice with similar combination effects; representative data is shown along with analysis using Combenefit software (Di Veroli et al., 2016). Synergy is tested for each drug concentration dose using the Lowe synergy model, and regions of dark blue within the 3D plots indicate dose combinations with strong synergistic effects, while regions of green are non-synergistic. Regions of red would indicate antagonism, however, none of the drug combinations evaluated demonstrated antagonism.

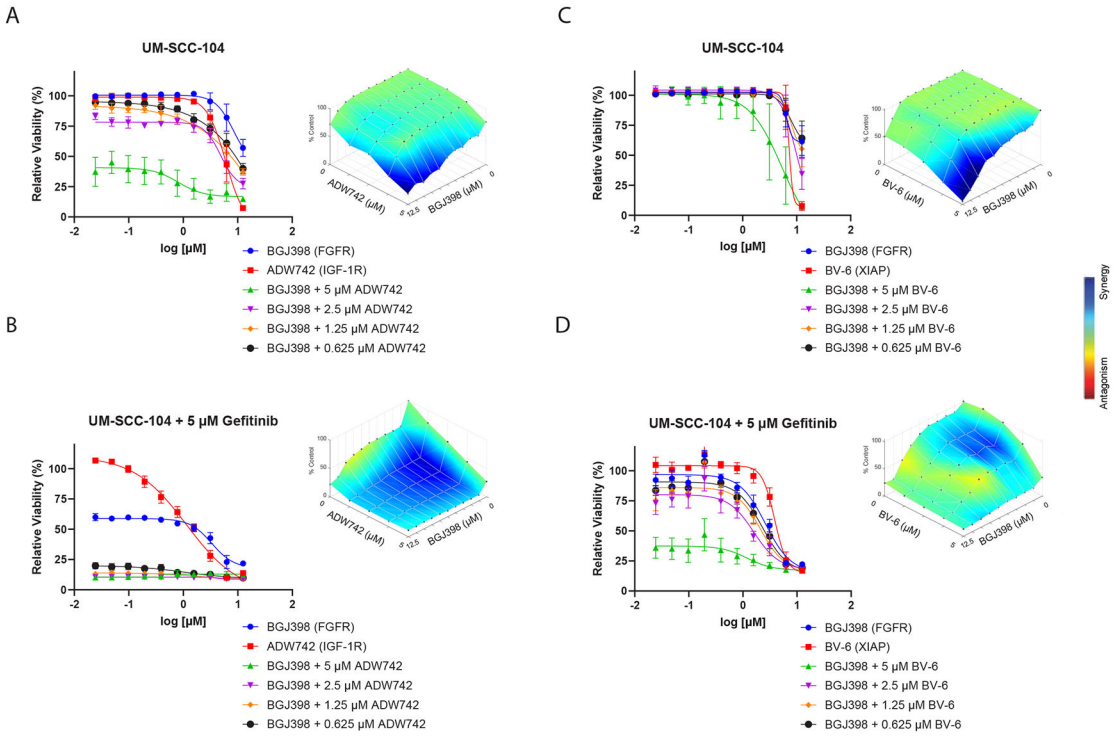

Figure 5. Effects of Combination Therapy Treatment in UM-SCC-104 cells.

UM-SCC-104 cells were treated with increasing concentrations of FGFR inhibitor BGJ398 and/or IGF-1R inhibitor ADW742 (**A**) or XIAP inhibitor BV-6 (**C**) for 72 hours. UM-SCC-104 cells were treated similarly in the presence of 5 μM gefitinib (**B, D**). Cell viability was measured using a resazurin cell viability assay. Each data point from dose-response curve is the mean and SD of quadruplicate determinations from a single experiment. Each experiment was repeated independently at least twice with similar combination effects; one representative data is shown by dose-response curve and two independent repeats are combined and shown by 3D plot after analysis using Combenefit software (Di Veroli et al., 2016). Regions of dark blue within the 3D plots indicate dose combinations with strong synergistic effects as in Figure 4. Of note, 0.195 μM BGJ398 and its corresponding BV-6 drug combinations with 5 μM gefitinib data points were removed from Combenefit analysis (**D**), because these data points cannot fit into its dose-response curve. Of note, viability data for BV-6/ADW742 from concentrations 0.625 μM, 1.25 μM, 2.5 μM and 5 μM are inferred from the dose-response curve after nonlinear regression by GraphPad Prism.